Benzotrithiophene-Based Hole-Transporting Materials for 18.2% Perovskite Solar Cells

Agustín Molina-Ontoria[+], Iwan Zimmermann[+], Inés Garcia-Benito, Paul Gratia,
Cristina Roldán-Carmona, Sadig Aghazada, Michael Graetzel,
Mohammad Khaja Nazeeruddin,* and Nazario Martín*

Abstract: *New star-shaped benzotrithiophene (BTT)-based hole-transporting materials (HTM) BTT-1, BTT-2 and BTT-3 have been obtained through a facile synthetic route by crosslinking triarylamine-based donor groups with a benzotri-thiophene (BTT) core. The BTT HTMs were tested on solution-processed lead trihalide perovskite-based solar cells. Power conversion efficiencies in the range of 16% to 18.2% were achieved under AM 1.5 sun with the three derivatives. These values are comparable to those obtained with today's most commonly used HTM spiro-OMeTAD, which point them out as promising candidates to be used as readily available and cost-effective alternatives in perovskite solar cells (PSCs).*

Since its first use as light absorber in a sensitized solar cell by Miyasaka and co-workers,[1] organic–inorganic methylammo-nium (MA) lead halide $MAPbX_3$ (X = I, Br) perovskites have experienced a scientific research blast for photovoltaic applications.[2–7] Organometal trihalide perovskites exhibit exceptional intrinsic properties such as light absorption from visible to near-infrared range, high extinction coefficient, long electron–hole diffusion lengths, a direct band gap as well as high charge carrier mobilities, among others.[8–10] Further-more, the perovskite material is relatively versatile and its electronic properties can be widely tuned by cationic or anionic substitution. As an example, the formamidinium (FA) based perovskite $FAPbI_3$ shows excellent light harvesting properties due to its lower band gap energy (E_g),[11] whereas by using the methylammonium mixed halide perovskite $MAPbI_xBr_{3-x}$ higher E_g and open circuit voltage (V_{oc}) can be obtained.[12] Improved energy conversion efficiencies are also observed when combining the two perovskite materials in the compositional modification $(FAPbI_3)_{1-x}(MAPbBr_3)_x$ that was recently presented by Seok et al.,[13] reporting power conversion efficiencies (PCEs) above 20%. The ambipolar behavior of the perovskite allows its combination either n–i–p or p–i–n configurations with electron transport-ing (ETMs) and/or with hole-transporting (HTMs) materials. These interface layers play an important role for transporting and blocking the charges. A wide number of HTMs have been synthesized and investigated in combination with perovskite absorber ranging from classical semiconducting polymers to small molecules.

Focusing on the latter, different central cores have been used in the state-of-the-art photovoltaic devices, such as 9,9′-spirobifluorene,[14] spiro-liked derivatives,[15] thiophene deriv-atives,[16] triphenylamine,[17] bridged-triphenylamines,[18,19] pyrene,[20] 3,4-ethylenedioxythiophene,[21] linear π-conju-gated,[22–24] triptycene,[25] tetraphenylethene,[26] silolothio-phene or triazines,[27] all of them namely decorated with diarylamines, triarylamines and/or carbazole derivatives. With this approach, the best power conversion efficiency obtained to date, up to 20%,[13] has been achieved by using the polymer poly[bis(4-phenyl)(2,4,6-trimethylphenyl)amine] (PTAA). According to their limited absorption in the visible region, these materials can act as hole-transporters without interfering the spectral response of the photoactive material. Nevertheless, there are also fewer examples of HTMs absorbing in the visible and near-infrared region, that is, by incorporating pentacene,[28] S,N-heteropentacene,[29] benzodi-thiophene derivatives,[30,31] phenoxazine[32] and thiolated nanographene,[33] and which exhibit PCEs over 15%. The low band-gap HTM layer enhances light absorption in the device, and exhibits beneficial effects. Actually, it has been previously reported that photons absorbed by low band-gap HTM results in a noticeable improvement of photocurrent.[34] In our case, the BTT series absorbs below 420 nm, where the perovskite strongly absorbs and, therefore, it has no influence on the solar cell efficiency.

Hitherto, the most studied HTM in PSC has been the 2,2,7,7-tetrakis(*N,N*-di-*p*-methoxyphenylamine)-9,9-spirobi-fluorene (Spiro-OMeTAD). Perovskite solar cells employing this semiconductor have achieved PCEs values over 19% by

[*] Dr. A. Molina-Ontoria,[+] I. Garcia-Benito, Prof. Dr. N. Martín
IMDEA-Nanociencia, C/ Faraday 9
Ciudad Universitaria de Cantoblanco, 28049 Madrid (Spain)
E-mail: nazmar@ucm.es

Dr. I. Zimmermann,[+] P. Gratia, Dr. C. Roldán-Carmona, S. Aghazada, Prof. Dr. M. K. Nazeeruddin
Group for Molecular Engineering of Functional Materials
Institute of Chemical Sciences and Engineering, EPFL VALAIS
1951 Sion (Switzerland)
E-mail: mdkhaja.nazeeruddin@epfl.ch

Prof. Dr. M. Graetzel
Laboratory of Photonics and Interfaces, Institute of Chemical Sciences and Engineering, EPFL VALAIS
1015 Lausanne (Switzerland)

Prof. Dr. N. Martín
Departamento Química Orgánica, Facultad C. C. Químicas
Universidad Complutense de Madrid
Av. Complutense s/n, 28040 Madrid (Spain)
Homepage: http://www.ucm.es/info/fullerene/

[+] These authors contributed equally to this work.

⚙ Supporting information for this article (detailed synthesis procedure, device preparation, additional SEM images, hysteresis curves, device statistics, detailed characterization including XRD, CV, DSC, TG, NMR, MS) can be found under:
http://dx.doi.org/10.1002/anie.201511877.

combining different strategies such as the interface engineering[35] between the charge transporting and extracting layers as well as by improving the formation of the perovskite crystal via the generation of a Lewis base adduct.[36] Unfortunately, the preparation of the spirobifluorene central core present in this material requires a complicated synthetic protocol which makes it a relatively expensive material. Besides, sublimation-grade of the Spiro-OMeTAD is an essential requirement in order to achieve high PCEs devices.[23]

In this work, we report a new family of ease to prepare HTMs based on a benzo[1,2-*b*:3,4-*b′*:5,6-*b″*]trithiophene (BTT) as a central core endowed with *p*-methoxydiphenyl-amine **(BTT-1)**, *p*-methoxydiphenylamine-substituted carbazole **(BTT-2)** and *p*-methoxytriphenylamine **(BTT-3)**. These compounds exhibit remarkable PCEs values when used in organometal trihalide perovskites solar cells (Figure 1). BTT
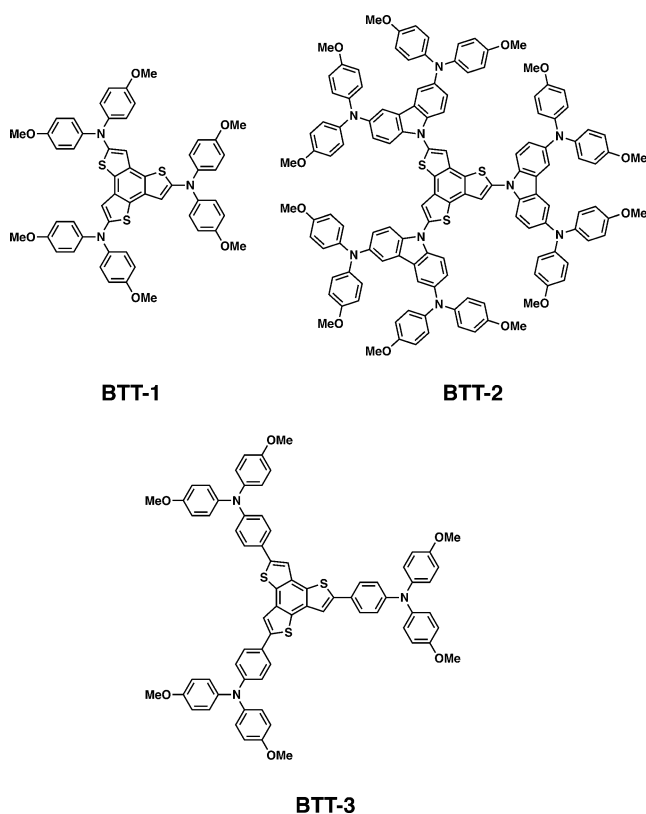

BTT-1   **BTT-2**

BTT-3

Figure 1. Chemical structures of **BTT-1**, **BTT-2** and **BTT-3**.

core exhibits a C_{3h} symmetry with three thiophene rings fused to a benzene central ring. The planarized star-shaped structure of the BTT is foreseen to promote an effective π–π intermolecular interaction, which could eventually lead to efficient hole-transporting properties.

The synthetic pathways and the experimental details for the preparation of the new family of HTMs are given in the Supporting Information (SI). The BTT central core was synthesized by a stepwise approach to obtain the tribromo-BTT, which involves the iodination of the 1,3,5-trichloroben-zene, Sonogashira cross-coupling reaction and ring closing reaction with sodium sulfide in NMP. In a subsequent

synthetic step, bromination of BTT by employing NBS leads to the formation of the desired tribromo-derivative. Finally, *p*-methoxydiphenylamine or *p*-methoxydiphenylamine-substituted carbazole were introduced by Buchwald–Hartwig amination reaction to obtain tri-substituted BTT derivatives **BTT-1** and **BTT-2**. On the other hand, *p*-methoxytriphenyl-amine units were covalently linked to the BTT core by a Suzuki cross-coupling reaction, affording **BTT-3**. The new compounds were obtained as stable solids in a good overall yield (see Supporting Information).

As previously mentioned, the new HTM molecules **BTT-1**, **BTT-2** and **BTT-3** together with spiro-OMeTAD as a reference were tested on perovskite-based solar cells. The energy levels of the HTM materials are shown in Figure 2. As
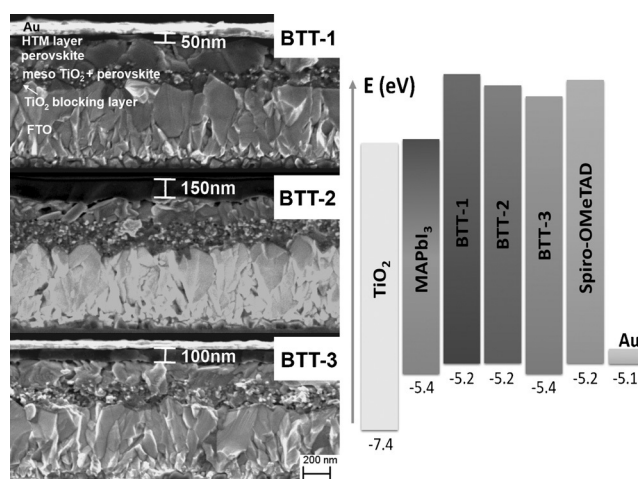

Figure 2. Left: Cross sectional images of devices fabricated with **BTT-1**, **BTT-2** and **BTT-3** on MAPbI₃ perovskite. The thickness of the hole-transporting layer is indicated. Right: Energy diagram of the different components in a perovskite solar cell.

can be observed in the Figure, the HOMO levels of the **BTT-1** and **BTT-2** molecules are very similar to the one for spiro-OMeTAD, whereas the **BTT-3** exhibits slightly lower HOMO level, which closely matches the energy level of the valence band edge of the MAPbI₃ perovskite. The cell architecture used in this study is shown among the high resolution scanning electron microscopy (SEM) cross-section images displayed in Figure 2. At the anode, a compact and meso-porous layer of TiO₂ was deposited on top of a fluorine-doped tin oxide (FTO) coated glass and used as the electron collector, while the cathode consists of a gold electrode thermally evaporated onto the HTM layer. The photoactive material MAPbI₃ is sandwiched in between these layers, as well as the modified perovskite (FAPbI₃)₀.₈₅(MAPbBr₃)₀.₁₅ recently introduced by Seok,[13] which was also tested for comparison. Both perovskite layers were fabricated by using a single step spin coating procedure similar to the protocol previously described in the literature.[37] As a summary, the perovskite precursor solution was spin-coated at 4000 rpm for 30 s. 10 s prior to the end of the spinning program, 120 μL of chlorobenzene were poured onto the spinning substrate to obtain a homogeneous dense perovskite film after annealing

for 1 h at 100°C. Compared to the standard perovskite devices, the composite material has a thicker capping layer of around 400 nm, three times larger than the value observed when using the standard perovskite. The hole-transporting materials presented in this study were then spin-coated on top of the perovskite layer at 4000 rpm for 15 s. The detailed procedure for the device fabrication is given in the SI.

The photovoltaic performance of the devices under AM 1.5 G conditions are shown in Figure 3 and the detailed results
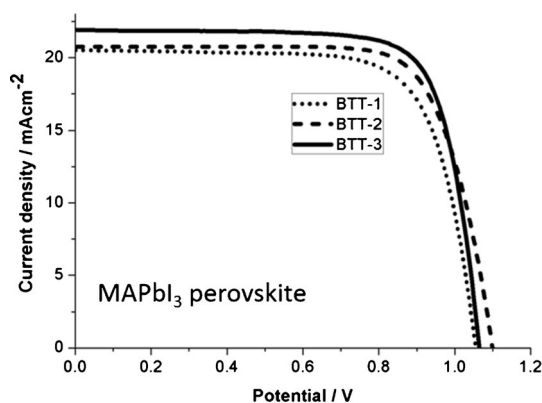
HTM	V_{oc} / mV	J_{sc} / mAcm^{-2}	FF / %	PCE / %
BTT-1	1043	20.4	72.3	16.0
BTT-2	1092	20.6	76.7	17.0
BTT-3	1065	21.9	76.7	18.2
spiro	1094	21.6	76.8	18.1
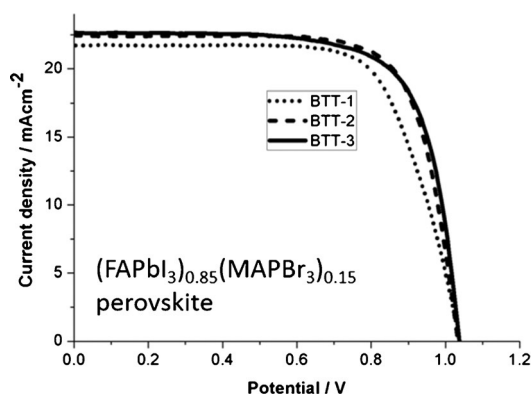
HTM	V_{oc} / mV	J_{sc} / mAcm^{-2}	FF / %	PCE / %
BTT-1	1039	21.6	70.6	16.0
BTT-2	1027	22.3	74.7	17.5
BTT-3	1037	22.7	72.4	17.3
spiro	1067	22.6	71.4	17.5

Figure 3. *I–V curves showing the performance of perovskite solar cells prepared by using* **BTT-1**, **BTT-2** *and* **BTT-3** *as HTM: standard MAPbI$_3$ perovskite (top) and compositional modified perovskite (FAPbI$_3$)$_{0.85}$-(MAPbBr$_3$)$_{0.15}$ (bottom). The J–V curves obtained for the reference can be found in the SI.*

are summarized in the table below. Current–voltage (*J–V*) curves were recorded by applying a forward bias with a scan rate of 10 mV s^{-1} in order to minimize the hysteresis effects stemming from the perovskite material.[38] Hysteresis scans showing the performance under forward and reverse bias can

be found in the SI. The results show excellent performances for all the benzotrithiophene derivatives, being **BTT-3** slightly better than its analogous **BTT-1** and **BTT-2**. Power conversion efficiencies (PCE) above 18.2% were observed on standard MAPbI$_3$ perovskite solar cells, with almost no hysteresis when tested under the described conditions. The average PCE of 17.7 ± 0.4% indicates a very good reproducibility for this molecule. Up to date such a high PCE value could be only achieved when using either spiro-OMeTAD or PTAA as hole-transporting materials. Comparing the results obtained for the three derivatives, the main difference when using **BTT-3** is the high short circuit current density ($J_{sc} = 21.9$ mA cm^{-2}). In fact these values are very close to those obtained with the spiro-OMeTAD reference. Devices with **BTT-2,** on the other hand, show a remarkably high open circuit voltage of almost 1.1 V, resulting in PCEs up to 17% (average: 15.6 ± 1.1%). **BTT-1** shows the lower performance, which might be also related to its low solubility in chlorobenzene compared to **BTT-2** and **BTT-3**, making it more difficult to obtain uniform films and reproducible results, which can be seen from the relatively high standard deviation on the average PCE value of 13.9 ± 1.5%. Nevertheless, PCE values of up to 16% are still possible to be obtained by using this molecule. Comparing the devices prepared with the composite perovskite (FAPbI$_3$)$_{0.85}$(MAPbBr$_3$)$_{0.15}$ and BTT-HTM molecules, the resulting performances are very similar. As previously observed, **BTT-1** is the least effective HTM, leading to lower fill factor and J_{sc}. On the contrary, compounds **BTT-2** and **BTT-3** behave similarly and excellent PCE values of up to 17.5% are obtained. As a general trend, the presented chemical structures seem to favor the formation of homogeneous thin films with a good morphology and conductivity, which lead to excellent fill factor values (FF > 70%) comparable to those obtained for spiro-OMeTAD. These experimental findings suggest a high carrier mobility in these new materials.

The electrical conductivity of the BTT-based thin films was measured in a lateral configuration between 2.5 μm spaced gold contacts. Thin films of the BTT molecules were deposited onto substrates having interdigitated gold electrodes by using the same procedure as for device preparation, adding 3 mol% of FK209 as a dopant in all of them. Figure 4 shows the comparison of the conductivity determined for the three derivatives. The values were extracted using a linear fit and Ohm's law. As can be observed in the inset of Figure 4, **BTT-1** exhibits the lowest conductivity (6.0×10^{-6} S cm^{-1}), followed by **BTT-2** (1.3×10^{-5} S cm^{-1}). The conductivity of **BTT-3** is the highest, reaching 2.79×10^{-5} S cm^{-1}. Although this value is still about one order of magnitude lower than that of Spiro-OMeTAD[23] it seems to be sufficient for obtaining a high performance when a thin HTM layer is used.

The trend in conductivity clearly supports the observation of the device performance obtained for the three different BTT molecules. The thickness of the individual BTT layers was adjusted to obtain the best efficiencies. According to the results, the lower conductivity of **BTT-1** requires a very thin layer in order to have a good performance. Values for the shunt resistance of the three derivatives, estimated from the slope close to short circuit current, are very similar for the
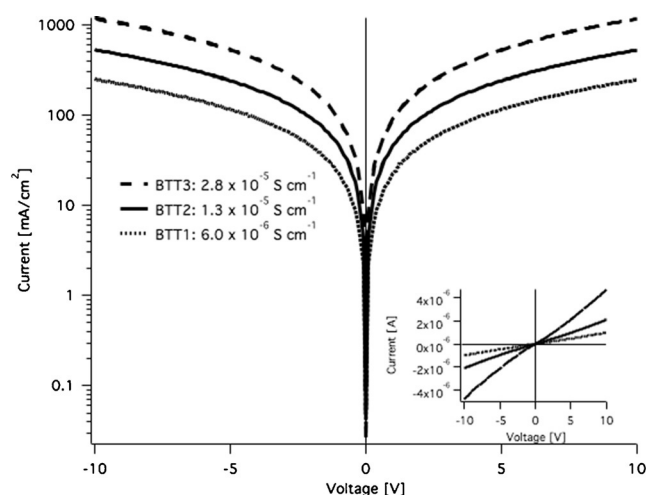
Figure 4. Lateral conductivity of the doped HTM molecules (**BTT-1**, **BTT-2** and **BTT-3**).

champion devices (> 2000 Ohm). Nevertheless, using a thinner HTM layer, it is more likely to generate shunting paths due to for example, roughness of the perovskite layer, which is reflected in the bad reproducibility of devices when employing thin (< 100 nm) HTM layers (see Supporting Information). Thicker HTM layers (> 100 nm) allowed a good reproducibility in BTT-3 devices.

In conclusion, three new star-shaped small molecule hole-conducting materials **BTT-1**, **BTT-2** and **BTT-3** have been efficiently obtained by crosslinking a benzotrithiophene (BTT) core with different triphenylamine based ligands following a facile straightforward synthetic route. The new compounds were employed in perovskite solar cells and showed excellent performances, comparable to the state-of-the-art perovskite based devices. Energy conversion efficiencies of up to 16% and 17% were obtained for **BTT-1** and **BTT-2**, respectively, and a PCE value above 18% for **BTT-3**, which is comparable to the reference spiro-OMeTAD. To the best of our knowledge, this is among the highest PCE values observed for PSC using a small molecule as an alternative to spiro-OMeTAD. The difference in the performance obtained for the three BTT derivatives could be accounted for by the different conductivity values obtained for the solid thin films. According to the results, the conductivity in **BTT-1** and **BTT-2** is considerably lower than that found for **BTT-3**, thus limiting the amount of current extracted from the device. Furthermore, compound **BTT-3** shows an excellent band alignment with the HOMO level of $MAPbI_3$ perovskite and, thus, it can be used as an efficient candidate for a cost-effective replacement of the widely established spiro-OMeTAD.

Acknowledgements

[1] A. Kojima, K. Teshima, Y. Shirai, T. Miyasaka, *J. Am. Chem. Soc.* **2009**, *131*, 6050.

[2] S. D. Stranks, P. K. Nayak, W. Zhang, T. Stergiopoulos, H. J. Snaith, *Angew. Chem. Int. Ed.* **2015**, *54*, 3240; *Angew. Chem.* **2015**, *127*, 3288.

[3] H. S. Jung, N. G. Park, *Small* **2015**, *11*, 10.

[4] H. S. Kim, C. R. Lee, J. H. Im, K. B. Lee, T. Moehl, A. Marchioro, S. J. Moon, R. Humphry-Baker, J. H. Yum, J. E. Moser, M. Graetzel, N. G. Park, *Sci. Rep.* **2012**, *2*, 591.

[5] M. M. Lee, J. Teuscher, T. Miyasaka, T. N. Murakami, H. J. Snaith, *Science* **2012**, *338*, 643.

[6] J. Burschka, N. Pellet, S. J. Moon, R. Humphry-Baker, P. Gao, M. K. Nazeeruddin, M. Graetzel, *Nature* **2013**, *499*, 316.

[7] M. Liu, M. B. Johnston, H. J. Snaith, *Nature* **2013**, *501*, 395.

[8] Y.-C. Hsiao, T. Wu, M. Li, Q. Liu, W. Qin, B. Hu, *J. Mater. Chem. A* **2015**, *3*, 15372.

[9] J. M. Ball, S. D. Stranks, M. T. Hörantner, S. Hüttner, W. Zhang, E. J. W. Crossland, I. Ramirez, M. Riede, M. B. Johnston, R. H. Friend, H. J. Snaith, *Energy Environ. Sci.* **2015**, *8*, 602.

[10] D. Shi, V. Adinolfi, R. Comin, M. Yuan, E. Alarousu, A. Buin, Y. Chen, S. Hoogland, A. Rothenberger, K. Katsiev, Y. Losovyj, X. Zhang, P. A. Dowben, O. F. Mohammed, E. H. Sargent, O. M.; Bakr, *Science* **2015**, *347*, 519; Bakr, *Science* **2015**, *347*, 519.

[11] W. S. Yang, J. H. Noh, N. J. Jeon, Y. C. Kim, S. Ryu, J. Seo, S. I. Seok, *Science* **2015**, *348*, 1234.

[12] S. Ryu, J. H. Noh, N. J. Jeon, Y. C. Kim, W. S. Yang, J. Seo, S. I. Seok, *Energy Environ. Sci.* **2014**, *7*, 2614.

[13] N. J. Jeon, J. H. Noh, W. S. Yang, Y. C. Kim, S. Ryu, J. Seo, S. I. Seok, *Nature* **2015**, *517*, 476.

[14] N. J. Jeon, H. G. Lee, Y. C. Kim, J. Seo, J. H. Noh, J. Lee, S. I. Seok, *J. Am. Chem. Soc.* **2014**, *136*, 7837.

[15] P. Ganesan, K. Fu, P. Gao, I. Raabe, K. Schenk, R. Scopelliti, J. Luo, L. H. Wong, M. Graetzel, M. K. Nazeeruddin, *Energy Environ. Sci.* **2015**, *8*, 1986.

[16] T. Krishnamoorthy, F. Kunwu, P. P. Boix, H. Li, T. M. Koh, W. L. Leong, S. Powar, A. Grimsdale, M. Graetzel, N. Mathews, S. G. Mhaisalkar, *J. Mater. Chem. A* **2014**, *2*, 6305.

[17] S. D. Sung, M. S. Kang, I. T. Choi, H. M. Kim, H. Kim, M. Hong, H. K. Kim, W. I. Lee, *Chem. Commun.* **2014**, *50*, 14161.

[18] P. Qin, S. Paek, M. I. Dar, N. Pellet, J. Ko, M. Graetzel, M. K. Nazeeruddin, *J. Am. Chem. Soc.* **2014**, *136*, 8516.

[19] H. Choi, S. Paek, N. Lim, Y. H. Lee, M. K. Nazeeruddin, J. Ko, *Chem. Eur. J.* **2014**, *20*, 10894.

[20] N. J. Jeon, J. Lee, J. H. Noh, M. K. Nazeeruddin, M. Graetzel, S. I. Seok, *J. Am. Chem. Soc.* **2013**, *135*, 19087.

[21] H. Li, K. Fu, A. Hagfeldt, M. Graetzel, S. G. Mhaisalkar, A. C. Grimsdale, *Angew. Chem. Int. Ed.* **2014**, *53*, 4085; *Angew. Chem.* **2014**, *126*, 4169.

[22] J. Wang, S. Wang, X. Li, L. Zhu, Q. Meng, Y. Xiao, D. Li, *Chem. Commun.* **2014**, *50*, 5829.

[23] P. Gratia, A. Magomedov, T. Malinauskas, M. Daskeviciene, A. Abate, S. Ahmad, M. Graetzel, V. Getautis, M. K. Nazeeruddin,

Angew. Chem. Int. Ed. **2015**, *54*, 11409; *Angew. Chem.* **2015**, *127*, 11571.

[24] B. Xu, E. Sheibani, P. Liu, J. Zhang, H. Tian, N. Vlachopoulos, G. Boschloo, L. Kloo, A. Hagfeldt, L. Sun, *Adv. Mater.* **2014**, *26*, 6629.

[25] A. Krishna, D. Sabba, H. Li, J. Yin, P. P. Boix, C. Soci, S. G. Mhaisalkar, A. C. Grimsdale, *Chem. Sci.* **2014**, *5*, 2702.

[26] L. Cabau, I. Garcia-Benito, A. Molina-Ontoria, N. F. Montcada, N. Martín, A. Vidal-Ferran, E. Palomares, *Chem. Commun.* **2015**, *51*, 13980.

[27] K. Do, H. Choi, K. Lim, H. Jo, J. W. Cho, M. K. Nazeeruddin, J. Ko, *Chem. Commun.* **2014**, *50*, 10971.

[28] S. Kazim, F. J. Ramos, P. Gao, M. K. Nazeeruddin, M. Graetzel, S. Ahmad, *Energy Environ. Sci.* **2015**, *8*, 1816.

[29] C. Steck, M. Franckevicius, S. M. Zakeeruddin, A. Mishra, P. Bauerle, M. Gratzel, *J. Mater. Chem. A* **2015**, *3*, 17738.

[30] Y. Liu, Q. Chen, H. S. Duan, H. Zhou, Y. Yang, H. Chen, S. Luo, T. B. Song, L. Dou, Z. Hong, Y. Yang, *J. Mater. Chem. A* **2015**, *3*, 11940.

[31] L. Zheng, Y. M. Chung, Y. Ma, L. Zhang, L. Xiao, Z. Chen, S. Wang, B. Qu, Q. Gong, *Chem. Commun.* **2014**, *50*, 11196.

[32] M. Cheng, C. Chen, X. Yang, J. Huang, F. Zhang, B. Xu, L. Sun, *Chem. Mater.* **2015**, *27*, 1808.

[33] J. Cao, Y. M. Liu, X. Jing, J. Yin, J. Li, B. Xu, Y. Z. Tan, N. Zheng, *J. Am. Chem. Soc.* **2015**, *137*, 10914.

[34] P. Qin, H. Kast, M. K. Nazeeruddin, S. M. Zakeeruddin, A. Mishra, P. Bauerle, M. Graetzel, *Energy Environ. Sci.* **2014**, *7*, 2981.

[35] H. Zhou, Q. Chen, G. Li, S. Luo, T. B. Song, H. S. Duan, Z. Hong, J. You, Y. Liu, Y. Yang, *Science* **2014**, *345*, 542.

[36] N. Ahn, D. Y. Son, I. H. Jang, S. M. Kang, M. Choi, N. G. Park, *J. Am. Chem. Soc.* **2015**, *137*, 8696.

[37] N. J. Jeon, J. H. Noh, Y. C. Kim, W. S. Yang, S. Ryu, S. I. Seok, *Nat. Mater.* **2014**, *13*, 897.

[38] W. Tress, N. Marinova, T. Moehl, S. M. Zakeeruddin, M. K. Nazeeruddin, M. Graetzel, *Energy Environ. Sci.* **2015**, *8*, 995.